BIOMOLECULES & THERAPEUTICS

Original Article
Biomol Ther, 648-658 (2017)

Calculation of a First-In-Man Dose of 7-*O*-Succinyl Macrolactin A Based on Allometric Scaling of Data from Mice, Rats, and Dogs

Keumhan Noh[1,Ψ] and Wonku Kang[2,*]

[1]*College of Pharmacy, Yeungnam University, Gyeongsan 38541,*
[2]*College of Pharmacy, Chung-Ang University, Seoul 06974, Republic of Korea*

Abstract

7-*O*-Succinyl macrolactin A (SMA) exerts several pharmacological effects including anti-bacterial, anti-inflammation, and anti-cancer activities. Recently, SMA has been extensively evaluated as an anti-cancer drug. Thus, the objectives of the present study were to characterise the pharmacokinetics of SMA via both non-compartmental and compartmental analysis in mice, rats, and dogs, and to derive an appropriate first-in-man dose based on allometric scaling of the animal data. The time courses of plasma SMA concentrations after intravenous administration to rats and dogs were analysed retrospectively, as were data collected after intraperitoneal SMA injection in mice. Pharmacokinetic parameters were estimated via both noncompartmental and compartmental analysis, and were correlated with body weight and/or the potential maximum life-span. The clearance and distribution volume of SMA in humans were predicted, and a first-in-man dose proposed. A two-compartment model best described the time courses of SMA plasma concentrations after a saturation elimination process was applied to fit the dataset obtained from rats. Incorporation of the maximum potential life-span during allometric scaling was required to improve the estimation of human clearance. The SMA clearance and the distribution volume in the steady state, in a 70-kg adult male, were estimated to be 30.6 L/h and 19.5 L, respectively. To meet the area under the curve (AUC) required for anti-tumour activity, a dose of 100 mg (~1.5 mg/kg) was finally proposed as the first dose for a 70-kg human. Although toxicological profiles derived from non-clinical studies must be considered before any final decision is made, our work will facilitate clinical studies on SMA.

Key Words: 7-*O*-Succinyl macrolactin A, Pharmacokinetics, First-In-Man dose, Allometric scaling, Dienetichron plot

INTRODUCTION

7-*O*-Succinyl macrolactin A (4-{[(3*Z*,5*E*,8*S*,9*E*,11*Z*,14*S*,16*R*,17*E*,19*E*,24*R*)-14,16-dihydroxy-24-methyl-2-oxo-1-oxacyclotetracosa-3,5,9,11,17,19-hexaen-8-yl]oxy}-4-oxobutanoic acid, SMA, Fig. 1) is a polyene macrolide containing a 24-member lactone ring, and is usually isolated from marine bacteria including *Streptomyces*, *Actinomadura*, and *Bacillus*. Recently, SMA was isolated at high yield from a fermentation broth of *Bacillus polyfermenticus* KJS-2 (Kim *et al*., 2009).

SMA exerts anti-bacterial effects against vancomycin-resistant enterococci (minimum inhibitory concentration [MIC], 2 mg/L) and methicillin-resistant Staphylococcus aureus (MIC, <0.25 mg/L). SMA was much more potent than teicoplanin,

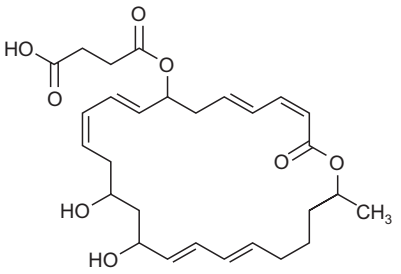

Fig. 1. Structure of 7-*O*-succinyl macrolactin A (SMA).

Open Access https://doi.org/10.4062/biomolther.2016.192

This is an Open Access article distributed under the terms of the Creative Commons Attribution Non-Commercial License (http://creativecommons.org/licenses/by-nc/4.0/) which permits unrestricted non-commercial use, distribution, and reproduction in any medium, provided the original work is properly cited.

Received Aug 24, 2016 **Revised** Dec 8, 2016 **Accepted** Jan 9, 2017
Published Online Mar 10, 2017

***Corresponding Author**
E-mail: wkang@cau.ac.kr
Tel: +82-2-820-5601, Fax: +82-2-816-7338

ΨPresent Address
Department of Pharmaceutical Sciences, Leslie Dan Faculty of Pharmacy, University of Toronto, 144 College Street, Toronto M5S 3M2, Canada

Copyright © 2017 The Korean Society of Applied Pharmacology

which is used to treat vancomycin-resistant enterococcal infections (Kim *et al*., 2011). SMA also exerts a protective effect on intestinal inflammation (Park *et al*., 2014). Recently, SMA was shown to exert significant anti-angiogenic effects on human umbilical vein endothelial cells, which may be attributable to inhibition of the vascular endothelial growth factor (VEGF)-induced angiogenic process, proliferation, tube formation, and invasion. Intraperitoneal injection of SMA into tumour-bearing mice (the CT26 mouse colon cancer allograft model) afforded dose-dependent anti-tumour activity, and the survival rate was significantly extended (Regmi *et al*., 2015). SMA has been modified via formation of the Tris salt to improve water solubility, and the safety of this formulation is being evaluated in non-clinical studies.

A major issue in drug development is determination of an appropriate safe commencement dose for humans. Allometric scaling is based on the facts that energy requirements and the rates of physiological processes are closely associated with body size. Such scaling has been useful to predict pharmacokinetic parameters, including the clearances, distribution volumes, and half-lives, of drug candidates in humans, using data derived from various animals (Mordenti, 1986; Obach *et al*., 1997; Lin *et al*., 1999; Khor *et al*., 2000; Kelley *et al*., 2001). Such an approach is particularly useful when putative anticancer agents have narrow safety margins.

The pharmacokinetic profiles of SMA in mice and rats were previously examined by other researchers (Kim *et al*., 2013; Jung *et al*., 2014). Our group also reported on the pharmacokinetic behaviour of SMA in rats and dogs, using a sensitive and validated method to examine drug stability in plasma (Kim *et al*., 2014; Noh *et al*., 2014). In the present work, we conducted a pharmacokinetic analysis of SMA in mice to explore differences in data from various laboratories, which may be attributable to the analytical methodology chosen, or differences in animal care. Pharmacokinetic datasets from mice, rats, and dogs were analysed retrospectively.

The principal aims of the current study were to explore the relationships between SMA pharmacokinetic parameters, and physiological factors, in mice, rats, and dogs; to model the time courses of plasma SMA concentrations via computational modelling; and, finally, to predict SMA pharmacokinetic parameters in humans and define an appropriate first-in-man dose for clinical trials.

MATERIALS AND METHODS

Materials

The Tris salt of SMA (purity, 98.4%) was supplied by Daewoo Pharm. Co. Ltd (Busan, Korea). Methaqualone (the internal standard, IS) and sodium fluoride (NaF) were purchased from Sigma (Seoul, Korea). Acetonitrile and methanol were obtained from Burdick & Jackson (Muskegon, MI, USA). All other chemicals and solvents were of the highest available analytical grade.

Animals

Pharmacokinetic studies were conducted in 25 male ICR mice (28-34 g). The animal room was maintained at a temperature of 23 ± 3°C, a relative humidity of 50 ± 10% with 10-20 air changes/h, and a light intensity of 150-300 Lux with a 12-h light/dark cycle. The study was approved by the Yeungnam University Animal Care and Use Committee (Gyeongsan, Korea). All animals used in this study were cared for in accordance with the principles outlined in the National Institutes of Health Guide for the Care and Use of Laboratory Animals.

Pharmacokinetic experiments

SMA salt dissolved in saline was administered to male ICR mice via single intraperitoneal injections (100 mg/kg). As described earlier, single intravenous injections were also given to 15 male Sprague-Dawley rats (10, 30, and 90 mg/kg) and three male beagle dogs (25 mg/kg). Blood samples were obtained from the retro-orbital plexus of mice (100 μL; 1-2 samples from each mouse) and from the jugular vein of rats (200 μL) and dogs (1 mL). To ensure SMA stability (Noh *et al*. 2014), samples were collected in heparinised tubes containing NaF (final concentration 1 mg/mL). Samples were collected at 2, 5, 10, 15, 30, 45, 60, 90 and 120 min following SMA administration in mice; at 2, 5, 10, 20, 30, 45, 60, 75, 90 and 120 min in rats; and at 2, 5, 15, 30, 45, 60, 90, 120, 180, 240 and 360 min in dogs. After centrifugation at 13,200 rpm for 10 min, plasma was separated and stored at -20°C.

Analytical method

Plasma concentrations of SMA were determined using a validated analytical method (Noh *et al*., 2014). Briefly, SMA was quantified with the aid of an API 4000 LC-MS/MS system (AB SCIEX, Framingham, MA, USA) equipped with an electrospray ionisation interface, and operating in the positive-ion mode. The compounds were separated on a reverse-phase column (ZIC® Hilic, 50×2.1 mm internal diameter, 5-μm particle diameter; Merck, Darmstadt, Germany) featuring a mobile phase (10 mM formic acid in water, methanol, and acetonitrile; 15:15:70 v/v/v). The column was heated to 40°C, and the flow rate was held at 0.3 ml/min using an HP 1260 series pump (Agilent, Wilmington, DE, USA). SMA was identified principally as the sodium adduct ion $[M+Na]^+$ at *m/z* 525.4, and the IS yielded primarily protonated molecules $[M+H]^+$ at *m/z* 251.1. The product ions were scanned in Q3 after collision with nitrogen in Q2 at m/z 406.7 and 132.1 for SMA and the IS, respectively. Quantification was achieved by selective monitoring of SMA sodium adducts or protonated precursor ions, and associated product ions, with derivation of the ratios of the areas under the peaks for each solution. Analytical data were processed with the aid of Analyst software (version 1.5.2, Applied Biosystems, Foster City, CA, USA).

The IS (150 μL; 1 ng/mL in methanol) was added to 30 μL of plasma, vortexed for 30 s, and centrifuged (13,200 rpm, 10 min). Next, a 3-μL aliquot of the supernatant was injected into the column. The lower limit of quantitation (LLOQ) was 20 ng/mL and plasma samples that were expected to contain high levels of SMA were diluted 20- or 100-fold with blank plasma (Noh *et al*., 2015, 2016).

Model-independent analysis

The SMA pharmacokinetic parameters were obtained via analysis of the time course of plasma concentrations in mice following single intraperitoneal injections of Tris SMA, and in rats and dogs following single intravenous injections. Model-independent pharmacokinetic parameters were calculated via non-compartmental analysis using WinNonlin® (version 2.1, Scientific Consulting, Palo Alto, CA, USA); the parameters derived included the maximum concentration (C_{max}), the time

to maximum concentration (T_{max}), the area under the plasma concentration-time curve from the time of dosing extrapolated to infinity (the AUC_{∞}), the total body clearance (CL), the distribution volume (V_d), and the terminal half-life ($t_{1/2}$) (Chiou, 1978). The pharmacokinetic parameters obtained from each rat and dog were expressed as means ± standard deviations. The naïve-pooled method was used to describe the pharmacokinetics of SMA in mice (Kim and Kang, 2013).

Model-dependent analysis

Population pharmacokinetic modelling was performed using the subroutine ADVAN13 and the first-order conditional estimation with interaction (FOCE-I) methods of NONMEM® (version 7.2; ICON Development Solutions, MD, USA) running Pirana® (version 2.8.2, ActiveState, Vancouver, Canada) (Bauer, 2011; Keizer *et al*., 2013). The SMA plasma concentration-time curves following single intraperitoneal injections of Tris SMA (100 mg/kg) were described using a two-compartment model featuring a first-order absorption and elimination. Based on a previous report by Jung *et al*. (2014), the absolute bioavailability (F) for the concentration-time curves was fixed at 0.2. The time courses of plasma SMA concentrations after intravenous administration of Tris SMA to rats and dogs were characterised by a two-compartment model with nonlinear elimination described by the Michaelis-Menten equation, and first-order elimination, respectively. Observations below the LLOQ were excluded from the population pharmacokinetic modelling analyses.

The inter-individual variabilities of pharmacokinetic parameters were derived using the following exponential error model:

$$P_i = \theta \times \exp(\eta_i)$$

where P_i is the parameter for the ith individual, θ the typical population value of the parameter, and η_i the random inter-individual effect with a mean of 0 and variance ω^2.

The residual variability of an SMA parameter was calculated using a modified model combining the additive and proportional error, as follows (Keizer *et al*., 2013):

$$W = \sqrt{\varepsilon_{add}{}^2 + \varepsilon_{pro}{}^2 \times C_{pred,ij}}$$

$$C_{obs,ij} = C_{pred,ij} + W$$

where $C_{obs,ij}$ and $C_{pred,ij}$ represent the observed concentration in the i-th individual, and j-th the predicted concentration in that individual, respectively. ε_{add} and ε_{pro} are the random residual errors, which were normally distributed with means of zero and variances σ^2.

Model evaluation

The final selected model was evaluated using goodness-of-fit plots, non-parametric bootstrap analysis, and a visual predictive check (VPC). The bootstrapping and VPC were conducted with the aid of the Perl-speaks-NONMEM (PsN) Toolkit (version 3.7.6), and the results visualised using the Xpose (version 4.4.1) module of the R® statistics package (version 2.15.2) (Lindbom *et al*., 2005; Keizer *et al*., 2013).

A new randomly sampled replicate of the original dataset was obtained via bootstrap analysis with replacement. The final population pharmacokinetic model was re-fitted to each bootstrap replicate individually; the process was repeated 1,000-fold using different random draws (Parke *et al*., 1999). Bootstrap runs for which minimisation was unsuccessful were excluded from further analysis. The medians and 90% confidence intervals (CIs) for all population parameters were obtained.

The predictive performance of the model was evaluated via a VPC featuring 1,000 simulations (Post *et al*., 2008; Bergstrand *et al*., 2011). The median and nonparametric 90% prediction intervals (the 5th-95th percentiles) derived from simulated plasma concentrations were used to assess the final model. The observed concentration data were graphically overlaid with the median values thereof, and the 5th and 95th percentiles obtained from the simulated concentration-time profiles.

Allometric scaling

The pharmacokinetic parameters of SMA obtained from mice, rats, and dogs were used to predict the human parameters, via simple allometric scaling. The relevant equation was:

$$Y = a \times W^b$$

where Y is the pharmacokinetic parameter of interest, W the body weight, and a and b the coefficient and exponent, respectively, of the allometric equation (Mahmood and Balian, 1996b). The allometric relationship may be linearised when plotted using log-log coordinates:

$$\log Y = \log(a) + b \times \log(W)$$

where $\log(a)$ is the y-intercept and b the slope of the relationship.

The total clearance, and the central and steady-state distribution volumes, estimated via compartmental analysis in mice, rats, and dogs, were used to predict these parameters in a human. Importantly, we used the total SMA clearance obtained via non-compartmental analysis in rats that received 30 mg/kg Tris SMA intravenously to predict the human clearance, because SMA elimination by rats was nonlinear as the dose rose. The mean value of each pharmacokinetic parameter and the mean species weight were plotted using log-log coordinates. A linear relationship was fitted to the log-transformed data to estimate the parameters a and b.

If necessary, the maximum potential life-span (MLP) and/or brain weight were/was incorporated into the equations, depending on the value of the clearance exponent derived via simple allometry.

Finally, the total clearance estimated by allometric scaling was used to predict the first-in-man dose of SMA. Clearance was multiplied by the AUC (~200 mg·min/L) to ensure sufficient anti-tumor activity (Kang *et al*., 2012).

Dedrick plots

Since intravenous administration of 10 and 30 mg/kg of SMA in rats and 25 mg/kg in dogs yielded linear pharmacokinetics, the SMA plasma concentration-time profiles were predicted using three Dedrick plots (Dedrick *et al*., 1970), including kallynochrons (elementary Dedrick plots), apolysichrons (complex Dedrick plots) (Boxenbaum and Ronfeld, 1983), and dienetichrons (Boxenbaum, 1983), following a single intra-

venous injection of Tris salt in humans (1.5 mg/kg). The plot equations were as follows:

Kallynochrons (elementary Dedrick plots):

$$\mathrm{Time_H} = \mathrm{Time_A} \times \left(\frac{W_H}{W_A}\right)^{1-b}$$

$$\mathrm{Conc_H} = \mathrm{Conc_A} \times \frac{\mathrm{Dose_H}}{\mathrm{Dose_A}} \times \frac{W_A}{W_H}$$

Apolysichrons (complex Dedrick plots):

$$\mathrm{Time_H} = \mathrm{Time_A} \times \left(\frac{W_H}{W_A}\right)^{c-b}$$

$$\mathrm{Conc_H} = \mathrm{Conc_A} \times \frac{\mathrm{Dose_H}}{\mathrm{Dose_A}} \times \left(\frac{W_A}{W_H}\right)^{c}$$

Dienetichrons:

$$\mathrm{Time_H} = \mathrm{Time_A} \times \left(\frac{\mathrm{MLP_H}}{\mathrm{MLP_A}}\right) \times \left(\frac{W_H}{W_A}\right)^{c-d}$$

$$\mathrm{Conc_H} = \mathrm{Conc_A} \times \frac{\mathrm{Dose_H}}{\mathrm{Dose_A}} \times \left(\frac{W_A}{W_H}\right)^{c}$$

where W is the body weight in kg. The subscripts H and A indicate human and animal, respectively. The superscripts b, c, and d are the exponents derived upon simple allometry of CL and V_{ss}; and allometry of CL×MLP, across rats and dogs, respectively. MLP is the maximum potential life-span in h, and dose is the intravenous dose of SMA in milligrams. The human concentration-time curves predicted by the Dedrick plots were used to calculate human pharmacokinetic parameters including CL, V_{ss}, and $t_{1/2}$ employing a two-compartment model weighted with the squared reciprocal of the predicted concentration ($1/y^2$), using WinNonlin® (version 2.1, Scientific Consulting). The goodness of curve fitting for all Dedrick plots was evaluated using the Akaike Information Criterion (AIC) and visual examination.

RESULTS

Non-compartmental analysis of SMA in mice, rats, and dogs

The mean SMA plasma concentration-time profiles in mice after a single intraperitoneal injection of 100 mg/kg of the drug salt are shown in Fig. 2A. The SMA pharmacokinetic parameters are listed in Table 1. SMA was rapidly absorbed, and the plasma concentration thereof decayed bi-exponentially. The peak concentration (C_{max}) was 24.8 mg/L at 5 min. The $t_{1/2}$ was approximately 18.2 min, and the V_d and total CL were 5.0 L/kg and 0.2 L/min/kg, respectively. The estimated AUC_∞ was 423.2 mg·min/L.

The mean plasma concentration-time profiles of SMA in rats after single intravenous injections of 10, 30, and 90 mg/kg of the drug salt are shown in Fig. 2B. The pharmacokinetic parameters of SMA are listed in Table 1. The plasma concentrations of SMA exhibited a bi-exponential decay profile, as in mice, and the mean half-lives and distribution volumes ranged from 14-25 min and 0.2-0.33 L/kg, respectively. The systemic clearance of SMA fell with increasing dose (0.049 ± 0.018, 0.034 ± 0.007 and 0.018 ± 0.002 L/min/kg, respectively), and the AUC_∞s increased exponentially (185.7 ± 71.1, 734.5 ± 177.6 and 3,992.3 ± 359.5 mg·min/L, respectively).

The mean plasma concentration-time profile of SMA in dogs after single intravenous injections of 25 mg/kg of the drug salt is shown in Fig. 2C. The pharmacokinetic parameters of SMA

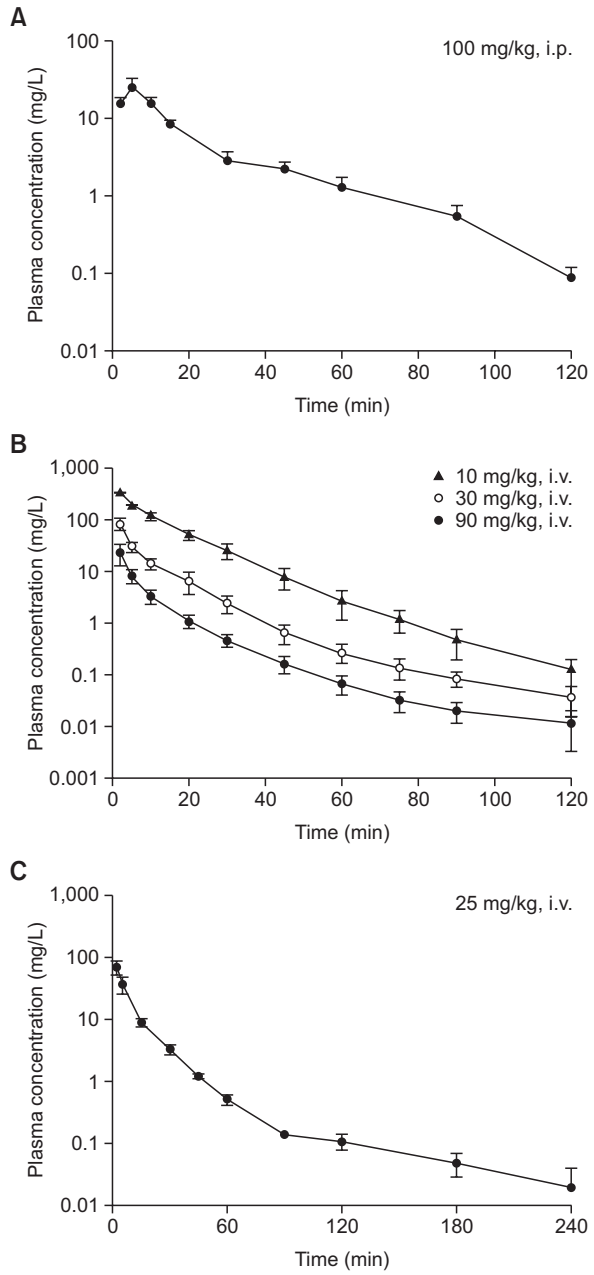

Fig. 2. The time courses of plasma SMA concentrations following intraperitoneal administration of 100 mg/kg of the Tris SMA salt to mice (A); intravenous administration of 10, 30, and 90 mg/kg of the salt to rats (B); and intravenous administration of 25 mg/kg of the salt to dogs (C) (means ± SDs; n=5).

Table 1. Model-independent SMA pharmacokinetic parameters following intraperitoneal (i.p.) or intravenous (i.v.) injection of the SMA Tris salt into mice, rats, and dogs

Parameter	Mice	Rats			Dogs
	100 mg/kg, i.p.	10 mg/kg, i.v.	30 mg/kg, i.v.	90 mg/kg, i.v.	25 mg/kg, i.v.
C_{max} (mg/L)	24.8	-	-	-	-
T_{max} (min)	5.0	-	-	-	-
$t_{1/2}$ (min)	18.2	17.0 ± 10.6	24.5 ± 10.2	14.1 ± 2.0	55.0 ± 19.2
V_d/F (L/kg)	5.0	0.33 ± 0.13	0.27 ± 0.06	0.20 ± 0.01	0.28 ± 0.03
CL/F (L/min/kg)	0.2	0.049 ± 0.018	0.034 ± 0.007	0.018 ± 0.002	0.026 ± 0.002
AUC_∞ (mg·min/L)	423.2	185.7 ± 71.1	734.5 ± 177.6	3992.3 ± 359.5	777.1 ± 65.5

Data are expressed as mean ± SDs (n=5), except for the naïve-pooled mean values obtained from three different mice.

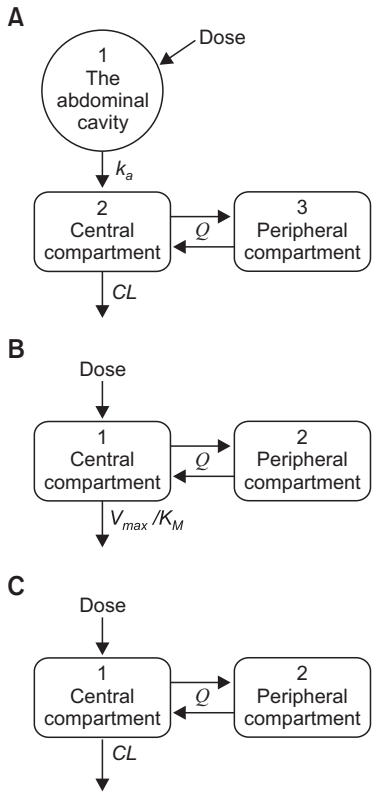

Fig. 3. Pharmacokinetic models of SMA in mice (A), rats (B), and dogs (C).

are listed in Table 1. As was also true of mice and rats, the plasma concentration of SMA decayed bi-exponentially, but the terminal half-life (55.0 ± 19.2 min) thereof was much longer in dogs than in the other animals. V_d and CL were 0.28 ± 0.03 L/kg and 0.026 ± 0.002 L/min/kg, respectively. The AUC_∞ was 777.1 ± 65.5 mg·min/L.

Compartmental analysis of SMA in mice, rats, and dogs

The time courses of plasma SMA concentrations were best described by a two-compartment model featuring linear elimination for mice (Fig. 3A) and dogs (Fig. 3B), and saturable elimination for rats (Fig. 3C).

Population pharmacokinetic analysis evaluated 45 SMA

Table 2. Estimates of population pharmacokinetic SMA parameters following intraperitoneal injection of the SMA Tris salt (100 mg/kg) into mice

Parameter	Estimate (%RSE[a])	Bootstrap median (95% CI[b])
Structural model		
k_a (h^{-1})	15.3 (7)	15.4 (9.2~19.9)
CL (L/h/kg)	2.39 (4)	2.39 (2.21~2.60)
V_2 (L/kg)	0.296 (9)	0.289 (0.179~0.408)
V_3 (L/kg)	0.384 (6)	0.380 (0.329~0.531)
Q (L/h/kg)	1.57 (14)	1.56 (1.15~2.23)
Inter-individual variability		
ω_{CL}	13.9% (21)	13.7% (5.0~19.1)
Residual error		
σ_{add} for SMA	0.0111 (16)	0.0144 (0.0019~0.1457)
σ_{prop} for SMA	0.216 (22)	0.189 (0.074~0.272)

[a]%RSE, relative standard error for estimate.
[b]CI, confidence interval calculated from 1000 bootstrap resamplings.

Table 3. Estimates of population pharmacokinetic SMA parameters following intravenous injection of the SMA Tris salt (10, 30, and 90 mg/kg) into rats

Parameter	Estimate (%RSE[a])	Bootstrap median (95% CI[b])
Structural model		
V_{max} (mg/h/kg)	260 (20)	266 (190~537)
K_m (mg/L)	78.1 (28)	80.1 (51.1~209.6)
V_1 (L/kg)	0.173 (14)	0.169 (0.130~0.216)
V_2 (L/kg)	0.201 (9)	0.198 (0.152~0.232)
Q (L/h/kg)	1.31 (20)	1.31 (0.85~1.80)
Inter-individual variability		
ω_{vmax}	14.6% (33)	13.5% (6.8~24.1)
Residual error		
σ_{add} for SMA	0.0466 (26)	0.0463 (0.0233~0.0796)
σ_{prop} for SMA	0.192 (15)	0.185 (0.130~0.235)

[a]%RSE, relative standard error for estimate.
[b]CI, confidence interval calculated from 1000 bootstrap resamplings.

plasma levels derived from 25 ICR mice. The final population pharmacokinetic parameters of SMA are shown in Table 2. The mean central (V_2) and peripheral (V_3) distribution volumes were 0.296 L/kg (RSE, 9%) and 0.384 L (RSE, 6%), respectively. The estimated k_a was 15.3 h^{-1} (RSE, 7%). *Q* and *CL* were estimated to be 1.57 L/h/kg (RSE, 14%) and 2.39 L/h/kg (RSE, 4%), respectively. The estimated *CL* value was similar to that obtained upon non-compartmental analysis that considered the bioavailability of SMA (20%). The CL inter-individual variability was ~14%.

Population pharmacokinetic analysis evaluated 141 SMA plasma levels derived from 15 rats. The final population pharmacokinetic parameters of SMA are shown in Table 3. The mean central (V_1) and peripheral (V_2) distribution volumes were 0.173 L/kg (RSE, 14%) and 0.201 L/kg (RSE, 9%), respectively. The V_{ss} (sum of V_1 and V_2) values were similar to those obtained via non-compartmental analysis. The *Q*, V_{max}, and K_m estimates were 1.31 L/h/kg (RSE, 20%), 260 mg/h/kg (RSE, 20%), and 78.1 mg/L (RSE, 28%), respectively. The inter-individual variability of V_{max} was ~15%.

Twenty-seven SMA plasma levels from three beagle dogs were subjected to population pharmacokinetic analysis. The final population pharmacokinetic parameters for SMA are shown in Table 4. The mean central (V_1) and peripheral (V_2) distribution volumes were 0.31 L/kg (RSE, 6%) and 0.108 L (RSE, 2%), respectively. The *Q* and *CL* estimates were 0.068 L/h/kg (3%) and 1.4 L/h/kg (6%), respectively. The estimated *CL* and V_{ss} (the sum of V_1 and V_2) were similar to those obtained via non-compartmental analysis. Inter-individual variabilities in parameters were neglected because the sample

Table 4. Estimates of population pharmacokinetic SMA parameters following intravenous injection of the SMA Tris salt (25 mg/kg) into dogs

Parameter	Estimate (%RSE[a])	Bootstrap median (95% CI[b])
Structural model		
CL (L/h/kg)	1.7 (6)	1.7 (1.5~1.9)
V_1 (L/kg)	0.31 (6)	0.31 (0.27~0.33)
V_2 (L/kg)	0.108 (2)	0.106 (0.079~0.111)
Q (L/h/kg)	0.068 (3)	0.068 (0.065~0.106)
Residual error		
σ_{prop} for SMA	0.288 (7)	0.275 (0.191~0.309)

[a]%RSE, relative standard error for estimate.
[b]CI, confidence interval calculated from 1000 bootstrap resamplings.

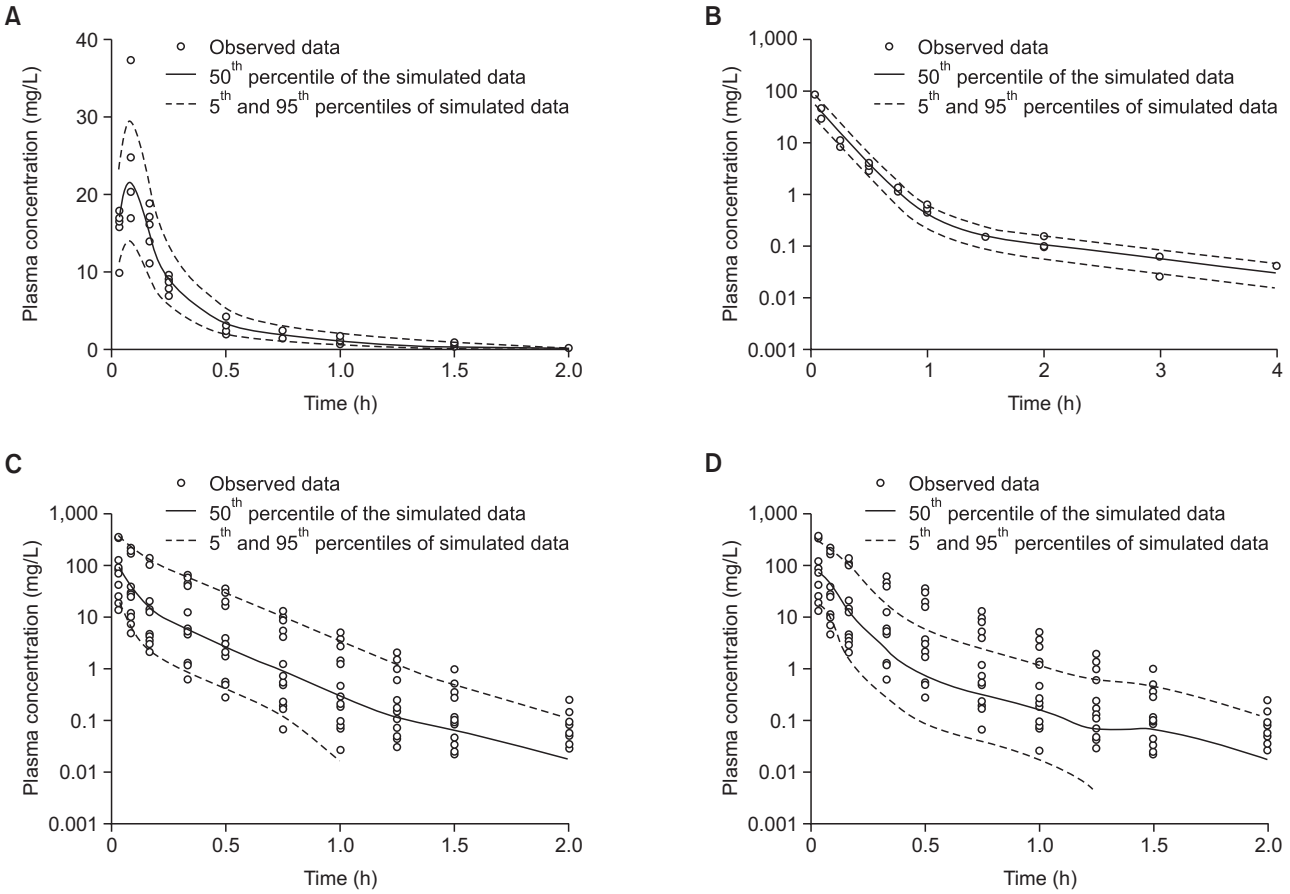

Fig. 4. Visual predictive check of the final model derived by injecting the SMA Tris salt into mice (A), dogs (B), and rats (C). Panel (D) shows a model fitted by linear elimination rather than the nonlinear process used to derive Fig. 4C. The solid, and upper and lower dashed, lines indicate the 50th, 95th, and 5th percentiles of the simulated data, respectively. The circles represent observational data.

Table 5. Allometric scaling of SMA pharmacokinetics based on data derived from mice, rats, and dogs

Parameter	Allometric equation	r^2	Predicted value in a 70 kg human (95% CI[a])	Method
CL (L/h)	$1.93\times(WT)^{0.9406}$	1.0000	104.9 (98.9~111.4)	Simple allometry
CL (L/h)	$10^{5.1476}\times(WT)^{1.2205}$/MLP	0.9990	30.6 (14.6~64.1)	CL×MLP
V_{ss} (L)	$0.45\times(WT)^{0.9236}$	0.9962	22.5 (7.4~69.0)	Simple allometry
V_c (L)	$0.26\times(WT)^{1.0208}$	0.9941	19.5 (4.2~91.6)	Simple allometry

[a]CI, confidence interval; WT and MLP represent body weight and maximum life-span potential, respectively.

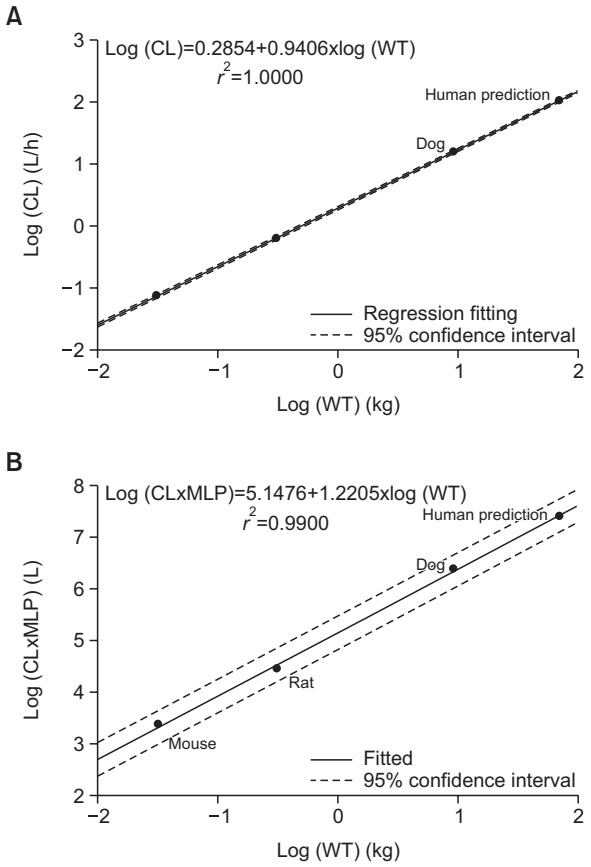

Fig. 5. Allometric scaling of SMA CL (A) and CL×MLP (B) versus species body weight (WT). The solid line represents the regression of the log-transformed data, and the dashed lines the 90% confidence intervals.

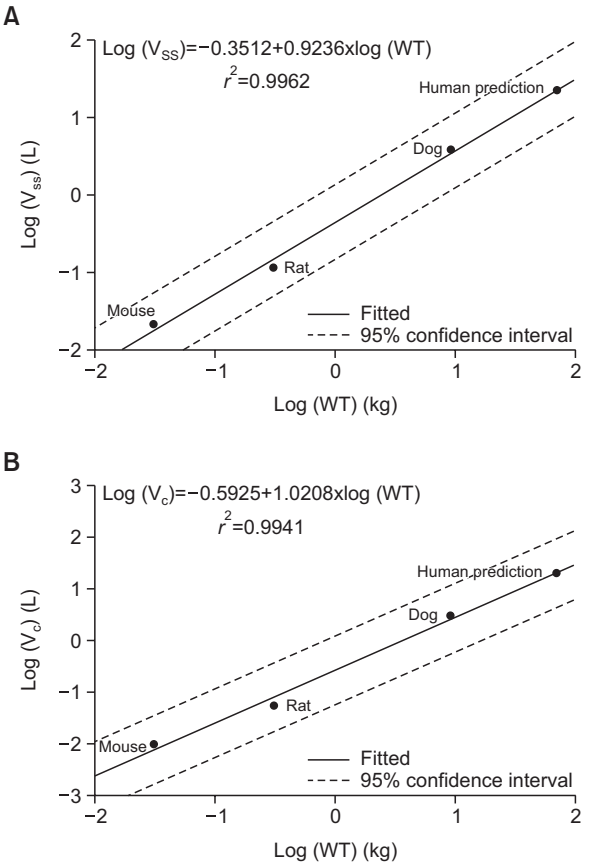

Fig. 6. Allometric scaling of SMA V_{ss} (A) and V_c (B) versus species body weight (WT). The solid line represents the regression of the log-transformed data, and the dashed lines the 90% confidence intervals.

size was small.

The observed bootstrap medians of SMA pharmacokinetic parameters were generally consistent with the mean population estimates. Basic goodness-of-fit plots for the final pharmacokinetic model showed that individually predicted SMA concentrations corresponded well to observations made in the absence of systemic bias, except for high drug concentrations in dogs. The conditional weighted predictions for the final population pharmacokinetic model were generally distributed around zero, and were relatively symmetrical (data not shown). The VPC results following single intraperitoneal injections into mice and single intravenous injections into dogs and rats are shown in Fig. 4A to 4C, respectively. Most observed concentrations were within the 90% prediction intervals (the 5th-95th percentiles), and were symmetrically distributed around the median, indicating that the model afforded good predictive performance. When a linear elimination process was incorporated into evaluation of the rat dataset, the time course of plasma SMA concentrations (especially after the 90 mg/kg dose) fitted poorly (Fig. 4D).

Allometric scaling

The results of allometric regression are listed in Table 5 and depicted in Fig. 5 and 6. The log-transformed pharmacokinetic parameters correlated well with the log-transformed body weights (r^2>0.994); and the estimated exponents for *CL*, V_{ss}, and V_c were 0.9406, 0.9236, and 1.0208, respectively. Using simple allometric scaling, the predicted values were 104.9 L/h

Table 6. Predicted SMA pharmacokinetic parameters following intravenous administration of 1.5 mg/kg of the SMA Tris salt to a human (70 kg), derived using Dedrick plots

Parameter	Kallynochrons	Apolysichrons	Dienetichrons
CL (L/h)	145.7 (104.1~187.4)[a]	148.0 (103.3~192.7)	38.7 (29.0~48.4)
V_{ss} (L)	27.3 (14.0~40.5)	19.2 (9.5~28.9)	20.2 (11.7~28.8)
$t_{1/2}$ (h)	0.31 (0.24~0.38)	0.22 (0.17~0.27)	0.88 (0.71~1.04)
AUC (mg·h/L)	0.6 (0.4~0.7)	0.6 (0.4~0.7)	2.2 (1.6~2.7)
AIC	-280.7	-277.4	-288.3

[a]Estimate (90% confidence interval), AIC, Akaike Information Criteria.

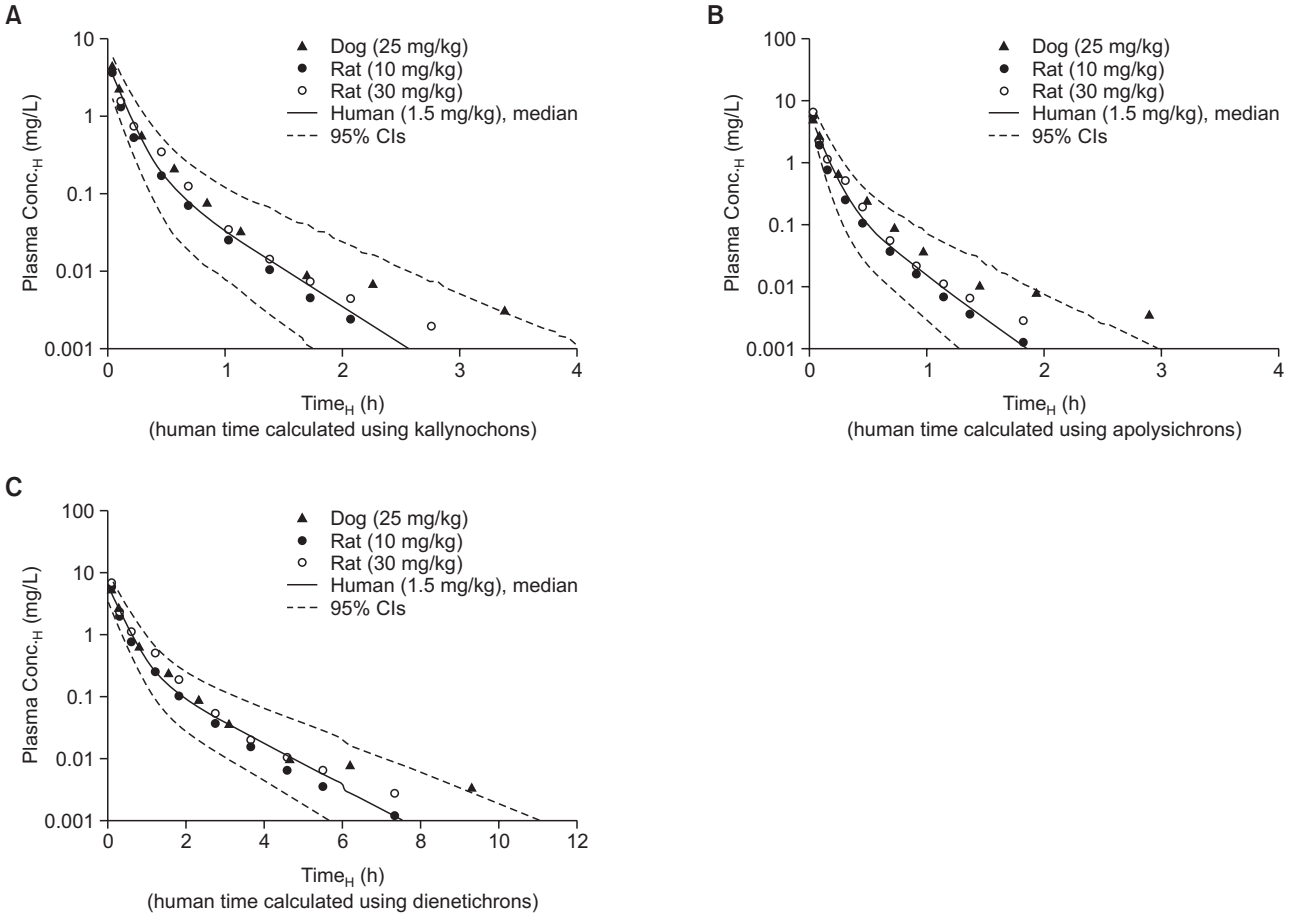

Fig. 7. The estimated plasma SMA concentration-time profile in humans following a single intravenous administration of 1.5 mg/kg of the SMA Tris salt. The data were obtained via concentration-time transformations using the pharmacokinetic time; and kallynochrons (A), apolysichrons (B), and dienetichrons (C). The solid line represents the regression of the log-transformed data, and the dashed lines the 90% confidence intervals (CIs).

for *CL*, 22.5 L for V_{ss}, and 19.5 L for V_c, in a 70-kg human. The estimated exponent for *CL* was 0.9406, indicating that the *CL* estimate was greater than the actual value (Mahmood and Balian, 1996b). Therefore, the rule of exponents function was used to improve the prediction performance (Mahmood and Balian, 1996b). Thus, the human *CL* was calculated by dividing by the human MLP (8.18×10^5 h) (Mahmood, 2007):

$$\mathrm{CL_{human}} = \frac{a \times W^b}{8.18 \times 10^5}$$

The MLP was obtained in years by the following equation:

$$\mathrm{MLP(years)} = 185.4 \times (\mathrm{BW})^{0.636} \times W^{-0.225}$$

After considering the MLP (Fig. 5B), the human *CL* was more accurately calculated as 30.6 L/h (0.51 L/min) in a 70-kg human. Thus, the proposed first-in-man dose for a 70-kg human would be 100 mg (~1.5 mg/kg), which was calculated by multiplying the AUC (200 mg·min/L) by the clearance (0.51 L/min).

Dedrick plots

The results of the Dedrick plots are listed in Table 6, and the predicted plasma concentration-time profile of SMA in humans following a single intravenous administration of 1.5 mg/kg of the drug salt is shown in Fig. 7; data from three Dedrick plots are displayed. The predicted SMA pharmacokinetic parameters based on both elementary and complex Dedrick plots were 145.7 and 148.0 L/h for *CL*, 27.3 and 19.2 L for V_{ss}, and 0.31 and 0.22 h for $t_{1/2}$, in a 70-kg human. All estimated values were similar regardless of whether elementary or complex Dedrick plots were prepared. The dienetichron plot predicted that *CL*, V_{ss}, and $t_{1/2}$ in a 70-kg human would be 38.7 L/h, 20.2 L, and 0.88 h, respectively.

DISCUSSION

Allometric scaling has been useful to define first-in-animal doses, especially in large animals. Such calculations use the values of major pharmacokinetic parameters (clearance and distribution volume) obtained in small experimental animals. However, the ultimate goal of interspecies pharmacokinetic scaling is to determine first-in man doses. The mathematical analysis is based on similarities between animals, and animals and humans, in terms of anatomy, physiology, and biochemistry. Such interspecies relationships are well-established; drug disposition and/or clearance can be simply scaled, using a power-law relationship, by species body weight, and the MLP and/or brain weight can be incorporated into the equations to improve interspecies correlations (Mordenti, 1986).

SMA is under investigation as an anti-cancer drug; non-clinical safety studies are currently in progress. In the present study, the time courses of plasma SMA concentrations in mice, rats, and dogs following intraperitoneal or intravenous administration of the Tris salt were analysed using both non-compartmental and compartmental approaches. Human pharmacokinetic SMA parameters were predicted via allometric scaling, and a first-in-man dose was finally derived.

As SMA exhibited promising anti-tumour activity upon repeated intraperitoneal administration (50 mg/kg) to tumour-bearing mice (Kang *et al*., 2012), and as the intraperitoneal bioavailability of SMA in mice is ~0.2 (Jung *et al*., 2014), the SMA dose for rats was increased from 10 mg/kg to 90 mg/kg, and a half-dose (25 mg/kg) was given to dogs, to obtain pharmacokinetic parameters. As shown in Table 1, the clearance in rats decreased, and systemic exposure to SMA (as reflected by the AUC) exponentially increased, with increasing doses, indicating saturation of drug metabolism and/or excretion. Therefore, a Michaelis-Menten-type elimination process was used in compartmental modelling; the model successfully described the time courses of plasma SMA concentrations at all tested doses. V_{max} and K_M were estimated to be 260 mg/h/kg and 78 mg/L, respectively, and the intrinsic clearance (V_{max}/K_M) was 3.3 L/h/kg (0.055 L/min/kg), comparable to the systemic clearance (0.04 L/min/kg). This explains why the drug bioavailability in rats was twice that (0.028 L/min/kg) in dogs. In contrast, no difference in the distribution volumes of the three different doses given to rats was evident (range, 0.20-0.33 L/kg), and the figure was similar to that in dogs (0.28 L/kg) (Table 1). The estimated distribution volume in rats (0.374 L/kg) in the steady-state (V_{ss}, the sum of the volumes in the central and the peripheral compartments) yielded by the compartmental model was similar to that (0.418 L/kg) in dogs. These values were similar to the sum of the plasma and extracellular fluid volumes in rats (0.328 L/kg) and dogs (0.328 L/kg), suggesting a limited distribution of SMA in tissues (Li and Corey, 2013). Although the mouse V_{ss} (0.68 L/kg) seemed to be greater than that of other animals, both intraperitoneal bioavailability and the naïve pooled data from different test animals must be considered. The pharmacokinetic parameters estimated via model-dependent analysis were robust, as shown by re-sampling of 1,000 bootstraps, and were generally consistent with those derived via non-compartmental analysis.

Table 5 shows the predicted *CL*, V_c, and V_{ss} values in a 70-kg human, derived via simple allometric scaling, using pharmacokinetic parameters estimated in mice, rats, and dogs. Please note that the rat clearance measured after administration of 30 mg/kg Tris SMA was used in allometric scaling, because higher SMA doses tended to saturate the drug metabolic and excretion systems. Log-transformed body weights correlated well with log-transformed pharmacokinetic parameters in all three species (r^2>0.994, Fig. 5, 6). Mahmood and Balian developed the 'Rule of Exponents' to allow of a better understanding of the relationship between body weight and *CL* (Mahmood and Balian, 1996a; Mahmood, 2007). Simple allometry (clearance= a×weight^b) predicts clearance precisely when the exponent b ranges from 0.55 to 0.7, but if the exponent ranges from 0.71 to 0.99 or 1.0 to 1.3, the MLP or brain weight should be included in modelling to better predict drug clearance in humans. As shown in Fig. 5, the exponent of the simple allometric equation was 0.9406, and the human clearance (CL_{human}) was thus predicted using *CL*×MLP values; the final figure was divided by the human MLP (8.18×10^5 h) (Mahmood, 2007). Based on the brain weight (BW) of each species (Davies and Morris, 1993; Cosson *et al*., 1997), SMA clearance in a 70-kg human was hypothesized to be 0.25 L/min (0.08-0.78 L/min, 90% CI).

V_{ss} and V_c in a 70-kg human were predicted to be 22.5 L (7.4-69.0 L, 95% CI) and 19.5 L (4.2-91.6 L, 90% CI) respectively, via simple allometric scaling; interspecies differences in distribution volumes are negligible once the data are normalised to body weight. The predicted human values of V_{ss} and V_c suggest that the distribution of SMA was limited to plasma and extracellular fluid (21.2 L; Li and Corey, 2013). These findings are also comparable to those of rats and dogs. Moreover, our unpublished data revealed a tissue-to-plasma SMA concentration ratio of <1, suggesting the limited distribution into tissues.

Although the roles of hepatic and renal SMA elimination have not been clearly defined, previous studies suggest that both are important factors (Jung *et al*., 2014). However, the estimated systemic CLs were lower than that of hepatic blood in mice (0.04 vs. 1.31 L/min/kg, respectively), rats (0.055 vs. 1.31 L/min/kg, respectively), dogs (0.028 vs. 0.73 L/min/kg, respectively), and humans (0.51 vs. 1.3 L/min, respectively, in a 70 kg human) (Brown *et al*., 1997). Thus, hepatic metabolism and/or biliary excretion may contribute to the overall metabolism of SMA due to its restricted liver uptake from systemic circulation. The total clearances for different species represent a satisfactory relationship, indicating that the data obtained in this study should be sufficient to predict the human clearance of SMA.

A proposed human dose may be calculated by multiplying the clearance by the AUC associated with the desired phar-

macological efficacy. SMA exhibited anti-tumour activity when intraperitoneally injected at 50 mg/kg into tumour-bearing mice (Regmi *et al*., 2015). In the present study, the AUC was 423 mg·min/L when the dose was 100 mg/kg, an AUC of 200 mg·min/L would be expected to reflect an effective dose. Consequently, a first-in-human dose of 100 mg (~1.5 mg/kg) would be appropriate, considering the expected clearance rate (0.51 L/min in a 70-kg human).

Smaller experimental animals (e.g., mice and rats) live shorter lives than do larger animals such as dogs and monkeys, and the former animals generally clear drugs more rapidly than do the latter. In contrast to chronological time, biological time differs among species, and drugs are removed at similar rates with reference to the latter type of time (Boxenbaum, 1982). The time courses of drug plasma concentrations obtained from different species may indicate that decay patterns differ over chronological time. However, if the time is transformed to pharmacokinetic (biological) time (by division by body weight and the exponents from the allometric equations yielding clearance and distribution volume), and the plasma concentrations normalised by division by dose and body weight, time courses in different animals may be superimposed, and exhibit similar decay profiles.

To explore plasma SMA concentration profiles in biological time, chronological time courses from different animals were transformed using three different species-invariant time methods: kallynochrons (elementary Dedrick plots), apolysichrons (complex Dedrick plots), and dienetichrons. The data were evaluated via two-compartment modelling featuring first- order elimination, and the pharmacokinetic parameters of SMA estimated. The first-in-man dose for a 70-kg human is suggested to be 100 mg (~1.5 mg/kg). Plots of dose-normalised plasma SMA concentrations versus transformed times, from rats and dogs, were superimposable (Fig. 7), and the dienetichron plot (Fig. 7C) that considered the MLP best described the transformed dataset, compared to the kallynochron and apolysichron plots, in terms of both AUCs and visual examination. The pharmacokinetic parameters (Table 6) yielded by the dienetichron plot were similar to those derived via allometric scaling.

In general, drug doses that are not associated with any observable adverse effects in experimental animals during the conduct of non-clinical toxicity studies are commonly used to estimate first-in-human doses for initial clinical trials (Food and Drug Administration, 2005); the maximum tolerable doses of anti-cancer agents may be preferred in this context (Paxton *et al*., 1990).

Although further work on possible SMA toxicities is under investigation, no significant adverse effect was evident following repeated 6-week intraperitoneal drug injections of 100 mg/kg (~ 20 mg/kg intravenous dose) into mice, where the dose was >13-fold higher than that predicted in humans. Therefore, the first-in-man dose that we suggest on the basis of efficacy would be reasonable and safe.

In conclusion, 100 mg of the 7-*O*-succinyl macrolactin A Tris salt for a 70-kg adult male (~1.5 mg/kg) is suggested to be an appropriate first human dose, derived from allometric scaling that incorporated the MLP, and that considered the need for effective anticancer activity. The drug clearance is estimated to be about 0.51 L/min in a 70-kg human. Although toxicological profiles derived from non-clinical studies must be evaluated before any final decision is reached, our data will aid clinical studies of SMA.

ACKNOWLEDGMENTS

This work was supported by the National Research Foundation of Korea (NRF) grant funded by the Korea government (MSIP) (No. 2015R1A5A1008958).

REFERENCES

Bauer, R. (2011) NONMEM User's guide, introduction to NONMEM 7.2.0. ICON Development Solutions, Maryland.

Bergstrand, M., Hooker, A. C., Wallin, J. E. and Karlsson, M. O. (2011) Prediction-corrected visual predictive checks for diagnosing nonlinear mixed-effects models. *AAPS J.* **13**, 143-151.

Boxenbaum, H. (1982) Interspecies scaling, allometry, physiological time, and the ground plan of pharmacokinetics. *J. Pharmacokinet. Biopharm.* **10**, 201-227.

Boxenbaum, H. (1983) Evolutionary biology, animal behavior, fourth-dimensional space, and the raison d'etre of drug metabolism and pharmacokinetics. *Drug Metab. Rev*. **14**, 1057-1097.

Boxenbaum, H. and Ronfeld, R. (1983) Interspecies pharmacokinetic scaling and the Dedrick plots. *Am. J. Physiol.* **245**, R768-R775.

Brown, R. P., Delp, M. D., Lindstedt, S. L., Rhomberg, L. R. and Beliles, R. P. (1997) Physiological parameter values for physiologically based pharmacokinetic models. *Toxicol. Ind. Health* **13**, 407-484.

Chiou, W.L. (1978) Critical evaluation of the potential error in pharmacokinetic studies of using the linear trapezoidal rule method for the calculation of the area under the plasma level--time curve. *J. Pharmacokinet. Biopharm.* **6**, 539-546.

Cosson, V. F., Fuseau, E., Efthymiopoulos, C. and Bye, A. (1997) Mixed effect modeling of sumatriptan pharmacokinetics during drug development. I: Interspecies allometric scaling. *J. Pharmacokinet. Biopharm.* **25**, 149-167.

Davies, B. and Morris, T. (1993) Physiological parameters in laboratory animals and humans. *Pharm. Res*. **10**, 1093-1095.

Dedrick, R., Bischoff, K. B. and Zaharko, D. S. (1970) Interspecies correlation of plasma concentration history of methotrexate (NSC-740). *Cancer Chemother. Rep.* **54**, 95-101.

Food and Drug Administration (2005) Guidance for industry: estimating the maximum safe starting dose in initial clinical trials for therapeutics in adult healthy volunteers. U.S. Department of Health and Human Services, Food and Drug Administration, Center for Drug Evaluation and Research (CDER).

Jung, J. W., Kim, J. M., Kwon, M. H., Kim, D. H. and Kang, H. E. (2014) Pharmacokinetics of macrolactin A and 7-O-succinyl macrolactin A in mice. *Xenobiotica* **44**, 547-554.

Kang, Y., Park, S., Kim, H. Y., Kim, D. H. and Kim, J. A. (2012) Inhibitory effects of macrolactin A and 7-O-succinyl macrolactin A on angiogenesis and cancer cell invasion. In Experimental Biology. San Diego Convent ion Center, San Diego.

Keizer, R. J., Karlsson, M. O. and Hooker, A. (2013) Modeling and simulation workbench for NONMEM: tutorial on pirana, PsN, and Xpose. *CPT Pharmacometrics Syst. Pharmacol.* **2**, e50.

Kelley, S. K., Harris, L. A., Xie, D., Deforge, L., Totpal, K., Bussiere, J. and Fox, J. A. (2001) Preclinical studies to predict the disposition of Apo2L/tumor necrosis factor-related apoptosis-inducing ligand in humans: characterization of in vivo efficacy, pharmacokinetics, and safety. *J. Pharmacol. Exp. Ther*. **299**, 31-38.

Khor, S. P., McCarthy, K., DuPont, M., Murray, K. and Timony, G. (2000) Pharmacokinetics, pharmacodynamics, allometry, and dose selection of rPSGL-Ig for phase I trial. *J. Pharmacol. Exp. Ther.* **293**, 618-624.

Kim, D. H., Kim, H. K., Kim, K. M., Kim, C. K., Jeong, M. H., Ko, C. Y., Moon, K. H. and Kang, J. S. (2011) Antibacterial activities of macrolactin A and 7-O-succinyl macrolactin A from *Bacillus polyfermenticus* KJS-2 against vancomycin-resistant enterococci and methicillin-resistant Staphylococcus aureus. *Arch. Pharm. Res.* **34**,

147-152.
Kim, E. and Kang, W. (2013) Pharmacokinetics of uridine following ocular, oral and intravascular administration in rabbits. *Biomol. Ther. (Seoul)* **21**, 170-172.
Kim, E., Shin, B., Kwon, K. I., Bang, J. S. and Kang, W. (2014) Simultaneous determination of 7-O-succinyl macrolactin A and its active major metabolite, macrolactin A in dog plasma using high-performance liquid chromatography with UV detection. *J. Sep. Sci.* **37**, 2833-2836.
Kim, J. M., Jung, J. W., Kim, D. H., Kang, J. S., Kim, C. G. and Kang, H. E. (2013) A simple and sensitive HPLC-UV determination of 7-O-succinyl macrolactin A in rat plasma and urine and its application to a pharmacokinetic study. *Biomed. Chromatogr.* **27**, 273-279.
Kim, K. M., Lee, J. Y., Kim, C. K. and Kang, J. S. (2009) Isolation and characterization of susurfactin produced by *Bacillus polyfermenticus* KJS-2. *Arch. Pharm. Res.* **32**, 711-715.
Li, J. J. and Corey, E. J. (2013) Drug discovery: practices, processes, and perspectives. Wiley & Sons, Inc.
Lin, Y. S., Nguyen, C., Mendoza, J. L., Escandon, E., Fei, D., Meng, Y. G. and Modi, N. B. (1999) Preclinical pharmacokinetics, interspecies scaling, and tissue distribution of a humanized monoclonal antibody against vascular endothelial growth factor. *J. Pharmacol. Exp. Ther*. **288**, 371-378.
Lindbom, L., Pihlgren, P. and Jonsson, E. N. (2005) PsN-Toolkit--a collection of computer intensive statistical methods for non-linear mixed effect modeling using NONMEM. *Comput. Methods Programs Biomed.* **79**, 241-257.
Mahmood, I. (2007) Application of allometric principles for the prediction of pharmacokinetics in human and veterinary drug development. *Adv. Drug Deliv. Rev*. **59**, 1177-1192.
Mahmood, I. and Balian, J. D.(1996a) Interspecies scaling: predicting clearance of drugs in humans. Three different approaches. *Xenobiotica* **26**, 887-895.
Mahmood, I. and Balian, J. D. (1996b) Interspecies scaling: predicting pharmacokinetic parameters of antiepileptic drugs in humans from animals with special emphasis on clearance. *J. Pharm. Sci.* **85**, 411-414.
Mordenti, J. (1986) Man versus beast: pharmacokinetic scaling in mammals. *J. Pharm. Sci.* **75**, 1028-1040.
Noh, K., Kim, D. H., Shin, B. S., Yun, H. Y., Kim, E. and Kang, W. (2014) Simultaneous determination of 7-O-succinyl macrolactin A and its metabolite macrolactin A in rat plasma using liquid chromatography coupled to tandem mass spectrometry. *J. Pharm. Biomed. Anal.* **98**, 85-89.
Noh, K., Nepal, M. R., Jeong, K. S., Kim, S. A., Um, Y. J., Seo, C. S., Kang, M. J., Park, P. -H., Kang, W., Jeong, H. G. and Jeong, T. C. (2015) Effects of baicalin on oral pharmacokinetics of caffeine in rats. *Biomol. Ther. (Seoul)* **23**, 201-206.
Noh, K., Oh, D. G., Nepal, M. R., Jeong, K. S., Choi, Y., kang, M. J., Kang, W., Jeong, H. G. and Jeong, T. C. (2016) Pharmacokinetic interaction of chrysin with caffeine in rats. *Biomol. Ther. (Seoul)* **24**, 446-452.
Obach, R. S., Baxter, J. G., Liston, T. E., Silber, B. M., Jones, B. C. MacIntyre, F., Rance, D. J. and Wastall, P. (1997) The prediction of human pharmacokinetic parameters from preclinical and in vitro metabolism data. *J. Pharmacol. Exp. Ther.* **283**, 46-58.
Park, S., Regmi, S. C., Park, S. Y., Lee, E. K., Chang, J. H., Ku, S. K., Kim, D. H. and Kim, J. A. (2014) Protective effect of 7-O-succinyl macrolactin A against intestinal inflammation is mediated through PI3-kinase/Akt/mTOR and NF-κB signaling pathways. *Eur. J. Pharmacol.* **735**, 184-192.
Parke, J., Holford, N. H. and Charles, B. G. (1999) A procedure for generating bootstrap samples for the validation of nonlinear mixed-effects population models. *Comput. Methods Programs Biomed.* **59**, 19-29.
Paxton, J. W., Kim, S. N. and Whitfield, L. R. (1990) Pharmacokinetic and toxicity scaling of the antitumor agents amsacrine and CI-921, a new analogue, in mice, rats, rabbits, dogs, and humans. *Cancer Res.* **50**, 2692-2697.
Post, T. M., Freijer, J. I., Ploeger, B. A. and Danhof, M. (2008) Extensions to the visual predictive check to facilitate model performance evaluation. *J. Pharmacokinet. Pharmacodyn.* **35**, 185-202.
Regmi, S. C., Park, S. Y., Kim, S. J., Banskota, S., Shah, S., Kim, D. H. and Kim, J. A. (2015) The anti-tumor activity of succinyl macrolactin A is mediated through the β-catenin destruction complex via the suppression of tankyrase and PI3K/Akt. *PLoS ONE* **10**, e0141753.